Hollow-core fiber Fabry-Perot photothermal gas sensor

FAN YANG,[1,2] YANZHEN TAN,[1,2] WEI JIN[1,2,*] YUECHUAN LIN,[1,2] YUN QI,[1] HOI LUT HO,[1,2]

[1]*Department of Electrical Engineering, The Hong Kong Polytechnic University, Hung Hom, Kowloon, Hong Kong, China*
[2]*Photonic Sensors Research Center, The Hong Kong Polytechnic University Shenzhen Research Institute, Shenzhen, 518057, China*
**Corresponding author: eewjin@polyu.edu.hk*

Received XX Month XXXX; revised XX Month, XXXX; accepted XX Month XXXX; posted XX Month XXXX (Doc. ID XXXXX); published XX Month XXXX

A highly sensitive, compact and low cost trace gas sensor based on photothermal effect in hollow-core fiber Fabry-Perot interferometer (FPI) is described. The Fabry-Perot sensor is fabricated by splicing a piece of hollow-core photonic bandgap fiber (HC-PBF) to single-mode fiber pigtails at both ends. Absorption of a pump beam in the hollow core results in phase modulation of probe beam, which is detected by the FPI. Experiments with a 2-cm-long HC-PBF with femtosecond laser drilled side-holes demonstrated a response time of less than 19 s and noise equivalent concentration (NEC) of 440 parts-per-billion (ppb) using 1 s lock-in time constant and the NEC goes down to 117 ppb (2.7×10^{-7} in absorbance) by using 77 s averaging time. © 2016 Optical Society of America

OCIS codes: *(060.0060) Fiber optics and optical communications; (060.2310) Fiber optics; (060.4005) Microstructured fibers; (060.5295) Photonic crystal fibers; (060.2370) Fiber optics sensors; (300.6430) Spectroscopy, photothermal.*

http://dx.doi.org/10.1364/OL.99.099999

Photothermal interferometry (PTI) has been exploited for trace gas detection and has demonstrated very high sensitivity and selectivity [1, 2]. A pump-probe configuration is typically used in which absorption of the pump beam results in localized heating, modulates refractive index and hence the phase of the probe beam, which can be detected by optical interferometry. The magnitude of the phase modulation is proportional to the absorption coefficient, the absorption distance, and the optical intensity (instead of power) of the pump [2]. Early PTI systems used free-space optics with gas or vapor cells up to a few tens of centimeters. The large diameter (>1 mm) of the free-space beam means high pump power on the level of several watts is needed in order to achieve detectable phase modulation [1]. With high power gas lasers operating in mid-infrared (e.g., CO_2 laser) where absorption is strong, gas detection down to ppb concentration level has been experimentally demonstrated [1]. These free-space systems are however complex, bulky, expensive and incompatible with fiber-optic systems.

Recently, we studied photothermal (PT) effect in gas-filled hollow-core photonic bandgap fibers (HC-PBFs) [3]. A HC-PBF confines gas or liquid phase materials and a propagating light mode simultaneously within its hollow core, and provides an ideal platform for light-gas interaction over a long distance [4, 5]. The diameter of the fundamental mode in a HC-PBF is typically 5-10 μm, more than two orders of magnitude smaller than a typical free-space beam, meaning that, for the same level of pump power, the pump intensity in a HC-PBF could be made significantly higher than a free-space beam. Hence the use of HC-PBF would enable significant level of phase modulation by use of a pump source with a relatively low power level and/or operating at a wavelength range with weaker absorption. This allows the use of laser sources and photonic components at the near-infrared wavelength range that are typically more cost-effective, compact and compatible with the standard telecommunication optical fiber systems. With a 10-m-long HC-PBF gas cell and a servo stabilized optical fiber Mach-Zehnder interferometer, we have demonstrated detection of acetylene gas down to 2 ppb [3], approximately three orders magnitude better than the previous direct-absorption optical fiber gas sensors.

In this paper, we report a PTI gas sensor with a miniature hollow-core fiber-based Fabry-Perot interferometer (FPI) as the probe interferometer. Compared with the Mach-Zehnder configuration in [3], the FPI sensor is simpler in design, smaller in size, much faster in response, avoids the use of active electronic servo stabilization, consumes less gas sample, and is more suitable for practical applications.

Figure 1(a) sketches the design of FPI gas cell. It is made by fusion splicing a 2-cm-long HC-PBF (HC-1550-06 from NKT Photonics) to standard single-mode fibers (SMF-28e from Corning) at both ends. The sensing HC-PBF has a hollow-core diameter of ~11 μm, a transmission window from 1500 to 1700 nm with a measured transmission loss of less than 16 dB/km at 1550 nm. This transmission band covers the absorption lines of a range of gases such as CO_2, CO, CH_4, N_2O, H_2S, NH_3, HI and C_4H_6, and could be used

to detect these gases [6]. There are other commercial HC-PBFs that have different transmission bands ranging from 400 nm to 2 μm, allowing a wider range of gases to be detected.

To facilitate gas-filling into the hollow core, two side-holes or micro-channels were fabricated by use of an 800-nm femtosecond laser [7], as shown in Fig. 1(a). The micro-channels are around the mid-point of the 2cm-long HC-PBF, giving a theoretical diffusion-limited response time of less than 10 seconds [8]. The femtosecond laser method for fabricating the micro-channels was described in [9], and the loss of the two micro-channels are less than 0.05 dB [3].

The two reflecting surfaces at the SMF/HC-PBF and HC-PBF/SMF joints, form a low-finesse FPI. For simplicity, we assume that the reflectivity at the two surfaces are approximately the same and equal to R (R<<1), and the coupling coefficient between the SMF and HC-PBF for the fundamental mode is α, neglecting the transmission loss of the HC-PBF, the reflected light intensity from the FPI may be approximated by [10],

$$I_R \approx I_0 R\left[1+\alpha^2+2\alpha\cdot\cos\varphi\right] \quad \textbf{(1)}$$

with

$$\varphi = \frac{4\pi n_{eff} d}{\lambda} + \varphi_0 \quad \textbf{(2)}$$

where I_0 and I_R are incident and reflected light intensity, φ is the phase difference between the two reflected beams, n_{eff} is the effective refractive index of the probe light, d is the cavity length, λ is the wavelength of the probe light, φ_0 is the constant phase shift. When a modulated pump beam is absorbed by the gas, n_{eff} and hence φ are modulated. We may therefore write, $\varphi = \varphi_{DC} + \varphi(t)$, with φ_{DC}

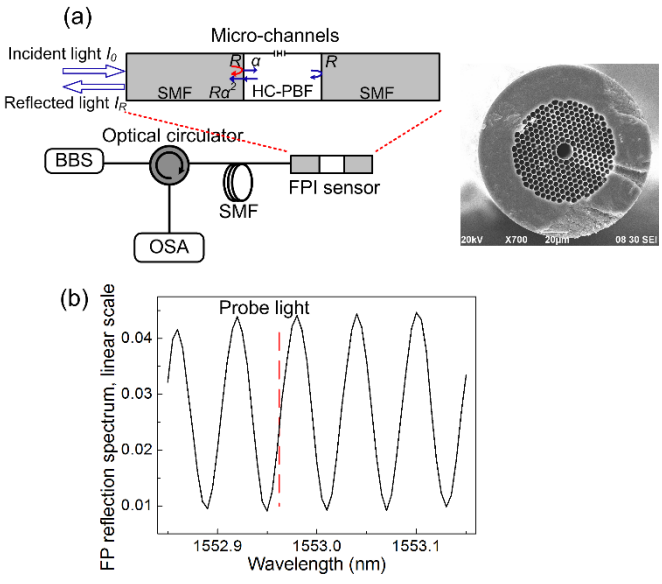

Fig. 1. (a) Setup for measuring the reflection spectrum of the hollow-core fiber gas cell and a typical cross section of a microchannel drilled on HC-PBF [9]. (b) The measured reflection spectrum. BBS, broadband source; OSA, optical spectrum analyzer.

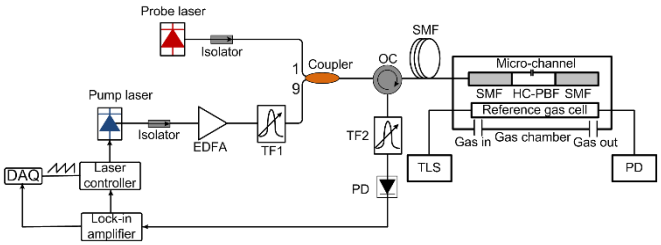

Fig. 2. Experimental setup for gas detection. EDFA, erbium-doped fiber amplifier; TF, tunable filter; OC, optical circulator; PD, photodetector; DAQ, data acquisition; TLS, tunable laser source. TF1 is used to minimize the EDFA's amplified spontaneous emission noise and TF2 to remove the pump light.

representing the DC phase offset and $\varphi(t)$ the photothermal phase modulation which is proportional to the gas concentration [3]. By properly selecting the operating wavelength, the interferometer can be operated around the quadrature point, i.e., $\varphi_{DC} \approx (m+1/2)\pi$, ($m$ is an integer).

The reflection spectrum of the gas cell was measured by using the setup shown in Fig. 1(a). A broadband optical source (Amonics, ALS-CWDM-FA) was used to illuminate the FPI, and the reflection spectrum was analyzed by an optical spectrum analyzer (OSA) via an optical circulator. The spectrum resolution and wavelength step or interval of the OSA were set to 10 pm and 5 pm respectively. Figure 1(b) shows the measured reflection spectrum. The wavelength spacing between adjacent fringes $\delta\lambda$ may be related to the cavity length d by $\delta\lambda \approx \lambda^2/2d$. For the 2-cm cavity length, $\delta\lambda$ is calculated to be 60.3 pm (at ~1553 nm), agreeing very well with the measured results shown in Fig. 1(b).

With the gas cell and the pump-probe setup shown in Fig. 2, we conducted gas detection experiments. The wavelength of the distributed feedback (DFB) semiconductor pump laser is sinusoidally modulated at 51 kHz and the mean wavelength is tuned to the P(9) absorption line of acetylene at 1530.371 nm. The periodic wavelength modulation results in periodic absorption and heating of the gas sample, modulating the phase of the probe beam. The processes of PT phase modulation occur in HC-PBF have been explained in [3]. The amplitude of the wavelength modulation was set to ~2.2 times the absorption linewidth in order to maximize the second-harmonic (2f) signal [3]. The FPI was probed by an external cavity diode laser (Agilent, 81600B) with its wavelength tuned to the steepest point in the reflection spectrum, i.e., 1552.96 nm as shown in Fig. 1(b). The reflected output of the FPI at the probe wavelength is demodulated by use of a lock-in amplifier (Stanford Research Systems, SR830). The gas cell was put into a 20cm×20cm×10cm gas chamber operating at atmospheric condition. An 8.7-cm-long fiber-pigtailed micro-optic open-path gas cell was also put into the gas chamber and used as a reference to estimate the gas concentration by directly measuring the attenuation of the transmitted light [11].

Figure 3(a) shows the second-harmonic lock-in outputs for different pump power levels delivered to the HC-PBF when the pump wavelength was tuned across the absorption line. The gas mixture was prepared by filling the gas chamber with 0.75% acetylene for ~10 seconds and then shut off the input and output valves of the chamber, and the gas concentration in the chamber is estimated to be 775 parts-per-million (ppm) acetylene. For the

pump power of 109.35 mW, the peak-to-peak amplitude of the 2f signal is 139.62 μV. The standard deviation of the noise was determined from the 2f lock-in output signal over a duration of 2 minutes when the pump wavelength was tuned away from the absorption peak to 1530.214 nm, and is about 0.079 μV, not much larger than the noise level when the pump is off (0.074 μV) and when the pump and probe are both off (0.06 μV).

Figure 3(b) shows the peak-to-peak amplitude of the 2f signal and the standard deviation of noise for different pump power levels. The signal amplitude increases approximately linearly with pump power while the noise level shows very little change. The signal-to-noise ratio (SNR) is calculated to be 1767 for the pump power of 109.35 mW and the corresponding 1σ minimum detection limit in terms of noise equivalent concentration (NEC) is 440 ppb for 1 s lock-in time constant with filter slope of 18 dB/Oct.

We also conducted an Allan deviation analysis [12, 13] based on the measured 2f signal over a one-hour period when the pump wavelength was tuned away from absorption peak to 1530.214 nm. The results are shown in Fig. 4. The Allan deviation decreases with the integration time according to the function $y = A/\sqrt{x} + B$ (the red fitted curve) and hence we may conclude that white noise dominates for short integration time of below ~100 seconds [13]. For averaging time of 77 seconds, the noise is 0.021 μV and the corresponding NEC is 117 ppb.

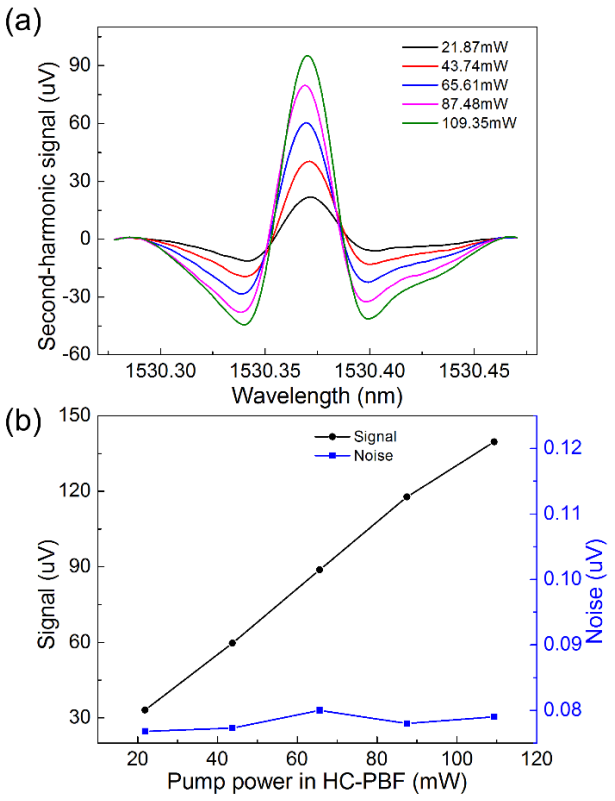

Fig. 3. (a) Second-harmonic signal spectrum with different pump power in HC-PBF. (b) Black curve: second-harmonic signal (peak-to-peak value) as function of pump power; blue curve: standard deviation of the 2f signal (noise) with duration over 2 minutes when the pump wavelength was tuned away from absorption peak to 1530.214 nm.

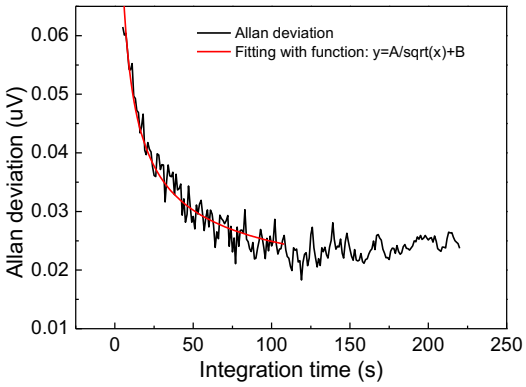

Fig. 4. Allan deviation plot of the sensor system with 775 ppm acetylene gas in HC-PBF. The black line is the Allan deviation calculation and the red line is the fitting result with function of $y = A/\sqrt{x} + B$.

A comparison with the results obtained previously from direct absorption spectroscopy, wavelength modulation spectroscopy and PTI with Mach-Zehnder interferometer are summarized in Table 1. The PTI systems obviously provided the best NEC of well below ppm level, and the performance of the Fabry-Perot configuration is impressive consider the short length of the HC-PBF used (2 cm). The performance of the current FPI systems in terms of noise equivalent absorbance (NEA) is 2.7×10^{-7} and ~1 order of magnitude better than that of the Mach-Zehnder configuration [3], probably due to longer integration time and larger pump power used in the study.

Table 1. Detection limits of different HC-PBF gas sensors.

Gas cell	Technique	NEC (ppm)	NEA
13.7 cm HC-PBF [14]	WMS	158 (CH_4)	2.5×10^{-4}*
5.1 m HC-PBF [15]	DAS	10 (CH_4)	8.2×10^{-4}
27 m HC-PBF [16]	DAS	50 (C_2H_2)	1.6×10^{-2}*
13 m HC-PBF [5]	WMS	1 (C_2H_2)	1.5×10^{-3}
10 m HC-PBF [3]	PTI	0.002 (C_2H_2)	2.3×10^{-6}
2 cm HC-PBF (this paper)	PTI	0.117 (C_2H_2)	2.7×10^{-7}

*Noise equivalent absorbance (NEA) data were calculated from noise equivalent concentration (NEC) data and the absorption line strength from HITRAN database [6]. WMS, wavelength modulation spectroscopy; DAS, direct absorption spectroscopy.

Figures 5(a) and (b) show the 2f lock-in outputs for concentration from 775 to 2900 ppm acetylene. These gas concentration levels were prepared by filling the gas chamber with 0.75% acetylene for different time and estimated using the open-path reference cell as mentioned before. When measuring each 2f signal for specific gas concentration, the inlet and outlet valves were shut and the gas concentration was kept stable. It shows the 2f signal increases approximately linearly with gas concentration and the dynamic range exceeds 2×10^4.

In our experiment, the volume of the gas chamber is relatively large, i.e, ~4 L (20cm×20cm×10cm), and it takes a long time for the

gas concentration in the chamber to reach that of the source gas [17]. This means that we could not test the response time of the gas cell by simply filling the chamber with different source concentrations, because the time taken to fill the chamber is much longer than the response time of the gas cell. To estimate the response time of the gas cell, we conducted the following tests: We use 0.75% acetylene gas balanced by nitrogen as source gas and tune the wavelength of pump laser to the peak of the absorption line. In the beginning, the gas chamber is full of atmospheric air. Then at 310 s, the gas is filled into the chamber with flow rate of ~300 sccm for ~10 s. After this process, the gas filling process is stopped and the gas inlet and outlet are shut. Figure 6 shows the change of the 2f signal during such a process. The output signal quickly becomes very stable after about 20 seconds, indicating the mixing of the gases in the chamber is fast and the C_2H_2 concentration in the gas cell and the chamber reaches a homogenous distribution, although the exact concentration of C_2H_2 within the cell is not determined. This procedure is repeated for two more times, and eventually the gas chamber is filled with high-purity nitrogen gas with ~300 sccm flow rate continuously.

From Fig. 6, we may estimate the response time of the gas cell. The time constant of the lock-in amplifier is 1 s with filter slope of 18 dB/Oct. As shown in the inset of Fig. 6, the rising time for 0-90% signal change is ~19 s. This rising time may be due to three different factors: the gas loading time that is ~10 s, the time taken for gas to mix in the chamber until it reaches a homogenous distribution, and the the response time of gas cell. Nevertheless, we may conclude that the response time of our gas cell is less than 19 seconds, which agrees with the theoretical analysis [7].

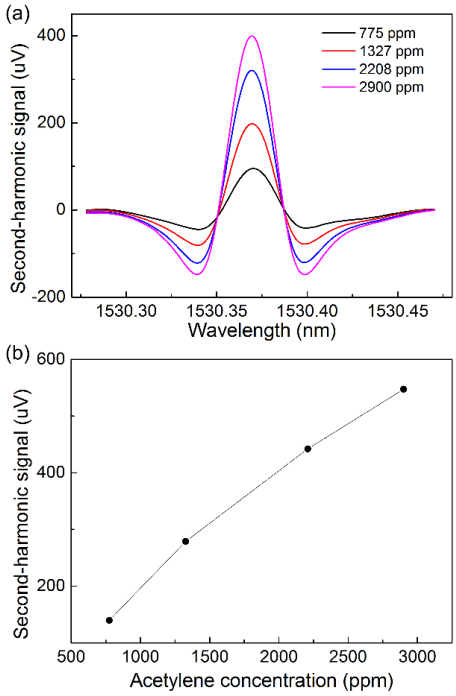

Fig. 5. 2f signal for different acetylene concentration. (a) 2f lock-in output when pump laser was tuned across the absorption line for 775, 1327, 2208, 2900 ppm acetylene; (b) 2f signal (peak-to-peak value) as function of gas concentration. The time constant of the lock-in amplifier is 1 s with filter slope of 18 dB/Oct.

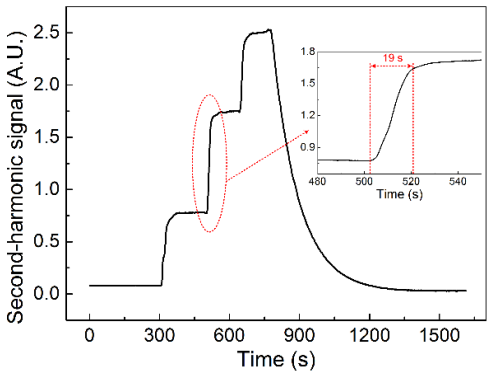

Fig. 6. 2f signal as function of gas loading when the pump wavelength was tuned to the absorption peak at 1530.371 nm.

In summary, we reported a novel compact sensing scheme based on photothermal effect in all-fiber HC-PBF FPI. The NEC is 440 ppb for 1 s lock-in amplifier time constant, and goes down to 117 ppb for 77 s averaging time. The response time of the sensor is less than 19 s. The shorter sensing HC-PBF will allow faster response as well as reduced volume of gas consumption. The realization of highly-sensitive fiber gas sensors with fast response would enable a range of important applications in environmental and air-pollution monitoring, in medicine (e.g., breath analysis) as well as in petrochemical industry.

Funding. the Hong Kong SAR government GRF grant (PolyU 152229/15E) and ITF grant (ITS/348/14), the National Natural Science Foundation of China (61290313), and The Hong Kong Polytechnic University grant 1-2VG4.

References

1. C. C. Davis and S. J. Petuchowski, Appl. Opt. **20,** 2539 (1981).
2. S. E. Bialkowski, Photothermal Spectroscopy Methods for Chemical Analysis (John Wiley & Sons, 1996).
3. W. Jin, Y. Cao, F. Yang, and H. L. Ho, Nat. Commun. **6,** 6767 (2015).
4. P. Russell, Science **299,** 358 (2003).
5. F. Yang, W. Jin, Y. Cao, H. L. Ho, and Y. Wang, Opt. Express **22,** 24894 (2014).
6. L. S. Rothman, I. E. Gordon, Y. Babikov, A. Barbe, D. Chris Benner, et al. J. Quant. Spectrosc. Radiat. Transf. **130,** 4 (2013).
7. Y. L. Hoo, S. Liu, H. L. Ho, and W. Jin, IEEE Photon. Technol. Lett. **22,** 296 (2010).
8. Y. L. Hoo, W. Jin, C. Shi, H. L. Ho, D. N. Wang, and S. C. Ruan, Appl. Opt. **42,** 3509 (2003).
9. W. Jin, H. L. Ho, Y. C. Cao, J. Ju, and L. F. Qi, Opt. Fiber Technol. **19,** 741 (2013).
10. B. Qi, G. R. Pickrell, J. Xu, P. Zhang, Y. Duan, W. Peng, Z. Huang, W. Huo, H. Xiao, R. G. May, and A. Wang, Opt. Eng. **42,** 3165 (2003).
11. Y. L. Hoo, W. Jin, H. L. Ho, J. Ju, and D. N. Wang, Sens. Actuators B **105,** 183 (2005)..
12. D. W. Allan, Proc. IEEE **54,** 221 (1966).
13. P. Werle, R. Miicke, and F. Slemr, Appl. Phys. B **57,** 131 (1993).
14. J. P. Carvalho, H. Lehmann, H. Bartelt, F. Magalhaes, R. Amezcua-Correa, J. L. Santos, J. Van Roosbroeck, F. M. Araujo, L. A. Ferreira, and J. C. Knight, J. Sensors **2009,** 398403 (2009).
15. A. M. Cubillas, M. Silva-Lopez, J. M. Lazaro, O. M. Conde, M. N. Petrovich, and J. M. Lopez-Higuera, Opt. Express **15,** 17570 (2007).
16. R. M. Wynne, B. Barabadi, K. J. Creedon, and A. Ortega, J. Lightwave Technol. **27,** 1590 (2009).
17. Y. Cao, W. Jin, H. L. Ho, L. Qi, and Y. H. Yang, Appl. Phys. B **109,** 359 (2012).